

Attitude Reference Generation for Spacecraft with Rotating Solar Arrays and Pointing Constraints

Riccardo Calaan
University of Colorado Boulder
3775 Discovery Drive
Boulder, CO, 80303
riccardo.calaon@colorado.edu

Cody Allard
Laboratory for Atmospheric and
Space Physics, 1234 Innovation Drive,
Boulder, CO, 80303
cody.allard@lasp.colorado.edu

Hanspeter Schaub
University of Colorado Boulder
3775 Discovery Drive
Boulder, CO, 80303
hanspeter.schaub@colorado.edu

Abstract—Advancements in space technology are enabling more sophisticated spacecraft designs with time-varying spacecraft configurations to account for varying power considerations. For example, articulating solar arrays that rotate about an axis fixed with respect to the hub can track the Sun at all times. Electric thrusters also have become omnipresent in modern spacecraft designs. Because these thrusters operate over long time windows, and the thrust vector must at all times be aligned with a specific inertial orientation, the optimal spacecraft attitude reference needs to accommodate the thruster too. Multiple pointing constraints pose a challenge to the attitude reference generation problem, because the attitude is characterized by three degrees of freedom, whereas the different constraints are often described by overdetermined systems of multiple equations. This paper leverages the different attitude parameterizations to provide a mathematical description of the solution space of the constraints outlined above. When the intersection space is nonzero it is possible to compute a solution that satisfies multiple constraints simultaneously. Conversely, an ordered list of pointing priorities is required in order to enforce the most important requirements, and reformulate the subsequent ones in terms of constrained optimization problems.

2014 respectively [4], [5], ESA’s Smart-1 mission, launched in 2003 [6], NASA’s Dawn mission, launched in 2007 [7], and the ESA-JAXA joint mission Bepi Colombo, launched in 2018 [8]. Another instance of deep-space mission that will involve electric propulsion is NASA’s Psyche mission, scheduled to launch in late 2023 [9]. Some of the more recent mission designs have explored the idea of mounting the electric thruster on a dual-gimbal mechanism that allows control of the direction of the thrust vector with respect to the spacecraft hub. In principle, this is motivated by the need to adjust the thrust direction based on the system’s center of mass, which changes location over time due to mass depletion [7], [10]. Recent studies [11] and mission designs [9] have explored the possibility of firing the dual-gimballed ET at an offset with respect to the system’s center of mass, in order to continuously dump the momentum accumulated on the system due to external perturbations.

Except for the Smart-1 and Bepi Colombo missions, which had the Moon and Mercury as their respective targets, all of the aforementioned missions involve the exploration of bodies in the asteroid belt. This marks the bottleneck for the applicability of EP to interplanetary missions, primarily due to the high power supply needed by the thruster to operate. In all of the above, power is supplied through solar arrays (SAs). However, the ability of the arrays to harvest solar power dramatically decreases with the distance from the Sun. As a consequence, solar energy is not a feasible option to power electric propulsion systems beyond the asteroid belt. Mission concepts exist that involve the exploration of the outer planets and their moons using radioisotope electric propulsion, where the thruster is supplied by radioisotope thermoelectric generators. Such mission designs remain, however, only theoretical at this stage [12], [13], [14]. Attitude is significantly impacted during the long time windows when an ET operates, because the thrust vector must at all times be aligned with a specific inertial orientation that is the result of trajectory planning.

Distance from the Sun is typically what regulates the sizing of the SAs. At large distances, these can reach up to 20 m² of surface area each [7]. However, another parameter severely affects the ability of the spacecraft to generate power: the inclination of sunlight with the power-generating surface of the array. For this reason, designs involving gimbaled SAs are becoming more and more common. Connecting the array to a one-axis gimbal gives an additional degree of freedom (DoF) that allows the array to track the direction of sunlight [3], [6], [15]. For hard-mounted arrays, in order to ensure maximum power generation, two out of three DoFs that describe the attitude are locked in order to have the arrays perpendicular to incident sunlight. Rotating SAs, instead, only require the rotation axis to be perpendicular to incident sunlight. This, in contrast, locks only one DoF.

TABLE OF CONTENTS

1. INTRODUCTION.....	1
2. POINTING REQUIREMENTS DEFINITION	2
3. INERTIAL POINTING WITH MAXIMUM POWER.....	3
4. INERTIAL POINTING WITH LOWER-BOUNDED POWER GENERATION	5
5. SOLAR ARRAY REFERENCE GENERATION	7
6. CONCLUSIONS.....	9
REFERENCES	9
BIOGRAPHY	10

1. INTRODUCTION

Recent advancements in spacecraft technology have enabled exciting new mission concepts to be designed. One such advancement that has slowly taken over the design for space missions is electric propulsion (EP), which has established itself as the leading technology for Earth-orbiting spacecraft first, and for missions to the inner Solar System later [1]. EP is characterized by a higher specific impulse, which means that an electric thruster (ET) can accelerate propellant to higher velocities, despite a smaller instantaneous thrust output, ultimately yielding a higher impulse-to-mass ratio [2].

Successful applications of electric thrusters in interplanetary missions are NASA’s Deep Space 1, launched in 1998 [3], JAXA’s Hayabusa 1 and 2 missions, launched in 2003 and

These multiple pointing constraints pose a challenge to the attitude reference generation problem. Attitude is characterized by three DoFs, and just the two pieces of equipment described lock, in total, several DoFs. Additionally, when the thrust direction in the body frame is time-varying, it is not trivial to determine whether multiple pointing constraints can be enforced simultaneously at all times. Moreover, spacecraft often present additional, softer constraints such as thermal-sensitive surfaces or equipment that must be kept away from the Sun, and which add another layer of complexity to the optimal attitude reference definition problem.

This paper leverages the Classic Rodrigues Parameters (CRP) attitude parameterization set to provide a rigorous mathematical description of the solution spaces of each type of constraint outlined above. Emphasis is given to the solution spaces for the constraints. In certain cases this intersection space is nonzero, and it is possible to compute a solution that satisfies multiple constraints simultaneously. Conversely, when such intersection space is empty, an ordered list of pointing priorities is required in order to enforce the most important requirement, and reformulate the subsequent ones in terms of constrained optimization problems. The ultimate goal of this paper is to provide a fully analytical formulation of the attitude reference generation problem as a function of spacecraft geometric properties and sensor measurements. This analytical formulation is used to deliver a closed-form solution that optimizes multiple requirements simultaneously and whose simplicity makes it suitable for on-board implementation.

This paper starts with Section 2, where the pointing requirements described above are defined analytically. Section 3 describes the space of admissible solutions when the desire is to apply all those requirements simultaneously, in order of priority. Section 4 builds on the results of Section 3 to describe how the solution space expands in the case that the tight power requirement can be relaxed. Section 5 describes how to generate the reference for the rotating solar arrays, also depending on the power requirements. Lastly, conclusions are drawn in Section 6.

2. POINTING REQUIREMENTS DEFINITION

The goal of this paper is to define a reference frame \mathcal{R} for the spacecraft, which satisfies a series of pointing requirements. The two-letter notation $[\mathcal{R}\mathcal{N}]$ describes the direction cosine matrix (DCM) that maps a vector from the inertial frame \mathcal{N} to the reference frame \mathcal{R} . The left superscript $^{\mathcal{B}}\hat{e}$ indicates the coordinate frame in which the vector \hat{e} is expressed, in this case the body-fixed frame \mathcal{B} . Each individual pointing requirement analyzed in this paper can be expressed as an inequality that describes the desired minimum or maximum angle between a certain unit direction vector in body/reference-frame coordinates, and another unit direction vector in inertial frame coordinates:

$$-1 \leq c_1 \leq {}^{\mathcal{R}}\hat{e}_1 \cdot [\mathcal{R}\mathcal{N}]^{\mathcal{N}}\hat{e}_2 \leq c_2 \leq 1. \quad (1)$$

The following types of pointing requirements, ordered by priority, are considered in this paper:

1. **Vector alignment:** this is the case in which, for example, the body-frame thrust direction must be aligned with an inertial requested direction. Alternatively, it can be the case where the body-fixed high-gain antenna (HGA) must be aligned along the direction of Earth relative to the spacecraft for telecommunication purposes. Referring with \hat{h}_1 to the

body vector, and with \hat{h}_{R1} to the inertial request vector, this requirement is expressed as:

$${}^{\mathcal{R}}\hat{h}_1 \cdot [\mathcal{R}\mathcal{N}]^{\mathcal{N}}\hat{h}_{R1} = 1, \quad (2)$$

where ${}^{\mathcal{R}}\hat{h}_1 = {}^{\mathcal{B}}\hat{h}_1$ under the assumption that the body frame will ultimately converge to the reference frame. This vector alignment alone locks two out of the three DoFs that characterize an attitude problem. Therefore, when present, it only leaves the space of rotations about the \hat{h}_{R1} axis to optimize for other potential pointing requirements.

2. **Solar array Sun incidence:** under the assumption of rotating solar arrays, this requirement is dictated by power requirements. Let's define \hat{s} as the unit direction vector of the Sun's position relative to the spacecraft, and with \hat{a} the unit direction of the solar array drive axis (SADA) in the body frame, about which the arrays can rotate. In the presence of two SAs whose drive axes are opposite with respect to one-another, it is sufficient to pick either as a valid description for \hat{a} without invalidating any of the results shown in this paper. The description does however fail when the SADAs are not collinear. The pointing requirement for the solar arrays is described by:

$$\left| {}^{\mathcal{R}}\hat{a} \cdot [\mathcal{R}\mathcal{N}]^{\mathcal{N}}\hat{s} \right| \leq \sin \gamma, \quad (3)$$

where γ indicates the incidence angle of sunlight, measured from the normal to the power-generating surface of the solar arrays, as shown in Figure 1. While it is out of the scope of this paper to go into the details of what the optimal γ is for the different phases of a space mission, it is relevant to acknowledge that this parameter is likely to vary depending on the relative position of the spacecraft and the Sun. Because irradiance decreases quadratically with the distance from the Sun [16], $\gamma \rightarrow 0$ is the desired outcome in outer regions of the Solar System. Substituting this condition into Equation (3) results in:

$${}^{\mathcal{R}}\hat{a} \cdot [\mathcal{R}\mathcal{N}]^{\mathcal{N}}\hat{s} = 0, \quad (4)$$

which is the condition for maximum power generation. This condition is equivalent to stating that the SADA must be perpendicular to the direction of incoming sunlight, and it locks one degree of freedom for the spacecraft attitude. In the inner regions of the Solar System it is possible to generate more power with suboptimal illumination conditions, due to the higher irradiance experienced by the spacecraft. In this

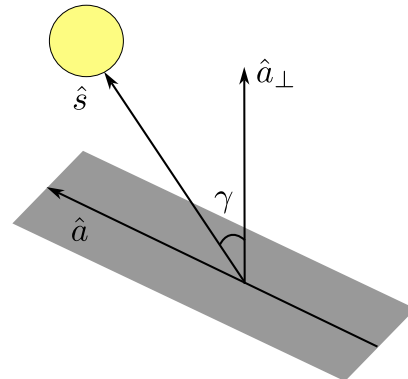


Figure 1: Sun incidence on array power-generating surface

case, the condition $0^\circ < \gamma < 90^\circ$ substituted into Equation (3) results in an even larger solution space, which can accommodate additional pointing requirements.

3. Keep-in/out zone: this third constraint is conceptually analogous to the first, but the alignment requirement is relaxed. This category describes a variety of requirements, such as thermally-sensitive surfaces or optical instruments that need to be kept at a certain angular distance from the Sun, or a low-gain antenna (LGA) that must point at Earth within an certain angular distance. The problem is formulated similarly, with a body-frame direction $\hat{\mathbf{h}}_2$, representing the instrument, and an inertial-frame direction $\hat{\mathbf{h}}_{R2}$ that describes the axis of the conical keep-in or keep-out zone. The pointing requirement is described by:

$${}^{\mathcal{R}}\hat{\mathbf{h}}_2 \cdot [{}^{\mathcal{R}\mathcal{N}}]{}^{\mathcal{N}}\hat{\mathbf{h}}_{R2} \geq \cos \theta, \quad (5)$$

where θ describes the half angle of the cone. Note that Equation (5) most intuitively describes a keep-in zone, but it can equivalently describe a keep-out zone when substituting $\hat{\mathbf{h}}_{R2}$ with the opposite vector $-\hat{\mathbf{h}}_{R2}$, and θ with $\pi - \theta$.

3. INERTIAL POINTING WITH MAXIMUM POWER

This subsection investigates the compatibility of requirements 1, 2, and 3, when applied simultaneously. This problem describes the case of a spacecraft like Psyche, where the thrust must be aligned at all times with the inertial requested vector, and at the same time the spacecraft must be able to generate as much power as possible. Additionally, it is desirable to point a thermally sensitive surface away from the Sun, to ensure heat dissipation. The requirements 1, 2, and 3 are therefore presented in order of importance.

The goal of this section is to define a reference frame \mathcal{R} that satisfies the pointing constraints. This is done by means of two consecutive rigid body rotations involving an intermediate frame \mathcal{D} :

$$[{}^{\mathcal{R}\mathcal{N}}] = [{}^{\mathcal{R}\mathcal{D}}][{}^{\mathcal{D}\mathcal{N}}]. \quad (6)$$

Thruster alignment

Enforcing requirement 1 is relatively straightforward. The principal rotation parameters (PRPs) are a set composed of a unit direction principal rotation vector (PRV) and a principal rotation angle (PRA), and they fully describe the relative attitude between two frames. For the intermediate frame DCM $[{}^{\mathcal{D}\mathcal{N}}]$ they are obtained as:

$${}^{\mathcal{N}}\hat{\mathbf{e}}_\phi = \frac{{}^{\mathcal{N}}\hat{\mathbf{h}}_1 \times {}^{\mathcal{N}}\hat{\mathbf{h}}_{R1}}{\left| {}^{\mathcal{N}}\hat{\mathbf{h}}_1 \times {}^{\mathcal{N}}\hat{\mathbf{h}}_{R1} \right|} \quad (7a)$$

$$\phi = \arccos \left({}^{\mathcal{N}}\hat{\mathbf{h}}_1 \cdot {}^{\mathcal{N}}\hat{\mathbf{h}}_{R1} \right), \quad (7b)$$

where the body-frame heading is preemptively mapped from current \mathcal{B} -frame coordinates to \mathcal{N} -frame coordinates. From Equation (7) the DCM $[{}^{\mathcal{D}\mathcal{N}}]$ is readily computed. See Ref. [17] for a full description of PRPs. The DCM $[{}^{\mathcal{D}\mathcal{N}}]$ so obtained describes a rotation from the inertial frame to a frame \mathcal{D} in which the pointing requirement on the thruster is satisfied.

Maximum power generation

The space of rotations about the thrust axis describes a set of frames, all compliant with the thruster pointing requirement. It is within this space that the second intermediate DCM $[{}^{\mathcal{R}\mathcal{D}}]$ is to be found, in order to maximize the incidence of sunlight on the solar arrays. The PRV for the second intermediate rotation $[{}^{\mathcal{R}\mathcal{D}}]$ coincides with the thruster heading:

$${}^{\mathcal{R}}\hat{\mathbf{e}}_\psi = {}^{\mathcal{R}}\hat{\mathbf{h}}_1 = {}^{\mathcal{R}}\hat{\mathbf{h}}_{R1}, \quad (8)$$

from which it is possible to define the CRP set (or Gibbs Vector):

$$\mathbf{q} = \tan \left(\frac{\psi}{2} \right) {}^{\mathcal{R}}\hat{\mathbf{e}}_\psi = t \cdot {}^{\mathcal{R}}\hat{\mathbf{e}}_\psi. \quad (9)$$

The expression of the DCM in terms of the CRP set is [17]:

$$[{}^{\mathcal{R}\mathcal{D}}] = \frac{((1 - \mathbf{q}^T \mathbf{q})[\mathbf{I}_{3 \times 3}] + 2\mathbf{q}\mathbf{q}^T - 2[\tilde{\mathbf{q}}])}{1 + \mathbf{q}^T \mathbf{q}}, \quad (10)$$

which is a function of the variable $t = \tan(\psi/2)$. Maximizing power generation is equivalent to requiring that the sunlight is perpendicular to the SADAs, or as close to perpendicular as possible. This translates into minimizing the expression on the left-hand side of equation Equation (3)

$$|f| = \left| {}^{\mathcal{R}}\hat{\mathbf{a}} \cdot [{}^{\mathcal{R}\mathcal{D}}][{}^{\mathcal{D}\mathcal{N}}]{}^{\mathcal{N}}\hat{\mathbf{s}} \right| = \left| {}^{\mathcal{R}}\hat{\mathbf{a}} \cdot [{}^{\mathcal{R}\mathcal{D}}]{}^{\mathcal{D}}\hat{\mathbf{s}} \right|. \quad (11)$$

Using the DCM expression in Equation (10), the quantity f can be expressed as:

$$f(t) = \frac{At^2 + Bt + C}{1 + t^2} \quad (12)$$

where:

$$A = 2 \left({}^{\mathcal{D}}\hat{\mathbf{s}} \cdot {}^{\mathcal{R}}\hat{\mathbf{e}}_\psi \right) \left({}^{\mathcal{R}}\hat{\mathbf{a}} \cdot {}^{\mathcal{R}}\hat{\mathbf{e}}_\psi \right) - {}^{\mathcal{D}}\hat{\mathbf{s}} \cdot {}^{\mathcal{R}}\hat{\mathbf{a}} \quad (13a)$$

$$B = 2 {}^{\mathcal{R}}\hat{\mathbf{a}} \cdot \left({}^{\mathcal{D}}\hat{\mathbf{s}} \times {}^{\mathcal{R}}\hat{\mathbf{e}}_\psi \right) \quad (13b)$$

$$C = {}^{\mathcal{D}}\hat{\mathbf{s}} \cdot {}^{\mathcal{R}}\hat{\mathbf{a}}. \quad (13c)$$

In Equation (13) it is, again, ${}^{\mathcal{R}}\hat{\mathbf{a}} = {}^{\mathcal{B}}\hat{\mathbf{a}}$ and ${}^{\mathcal{R}}\hat{\mathbf{e}}_\psi = {}^{\mathcal{B}}\hat{\mathbf{e}}_\psi$, assuming that the body frame will eventually converge to the reference frame. The coefficients A , B , and C are not entirely independent from one-another. C is the scalar product between two direction vectors, therefore it is:

$$-1 \leq C \leq 1. \quad (14)$$

B is two times the triple product of three unit direction vectors, which is known to be equal to the volume of parallelepiped which has such vectors as its sides. Because the angle between two of these vectors is already bound by C , it is:

$$-2\sqrt{1 - C^2} \leq B \leq 2\sqrt{1 - C^2}. \quad (15)$$

Lastly, A is bound by functions of both B and C , due to the scalar products that appear in its formulation. It can be proved that:

$$\frac{B^2}{2} - C - 2 \leq A \leq 2 - C - \frac{B^2}{2}. \quad (16)$$

The denominator in Equation (12) is never zero, making the expression always nonsingular, and the numerator is a

quadratic expression. Different types of solutions are sought depending on the discriminant $\Delta = B^2 - 4AC$ of this quadratic expression:

- $\Delta \geq 0$: the equation $f(t) = 0$ has two solutions. This means that maximum power condition is achievable, with incoming sunlight exactly perpendicular to the solar arrays' power-generating surface. The corresponding principal rotation angles (PRA) are obtained as:

$$\psi_{1/2} = 2 \arctan \left(\frac{-B \pm \sqrt{B^2 - 4AC}}{2A} \right). \quad (17)$$

- $\Delta < 0$: the equation $f(t) = 0$ has no real solutions. The optimal attitude is given by the PRA for which $|f(t)|$ is minimum. To find such value, let's consider the derivative of $f(t)$ with respect to t :

$$f'(t) = \frac{-Bt^2 + 2(A - C)t + B}{(1 + t^2)^2}. \quad (18)$$

The absolute minimum and maximum for the expression $f(t)$ are found equating $f'(t)$ to zero, which gives the two solutions:

$$\psi_{1/2} = 2 \arctan \left(\frac{A - C \pm \sqrt{(A - C)^2 + B^2}}{B} \right). \quad (19)$$

Note that the term under the square root in Equation (19) is always non-negative, therefore the two solutions are always real. In this case, however, the two solutions ψ_1 and ψ_2 are not equivalent: one corresponds to the maximum for $f(t)$, and the other one to the minimum. In order to maximize power generation, only the solution for which $|f(t(\psi))|$ is minimum should be chosen.

The optimal value for ψ can be combined into Equations (9) and (10) in order to compute $[\mathcal{R}\mathcal{D}]$, and ultimately the DCM between inertial frame and optimal reference $[\mathcal{R}\mathcal{N}]$.

Attention should be paid to the fact that there is no a priori knowledge on the coefficients A , B , and C , and while their definition is always nonsingular, singularities can be encountered in Equations (17) and (19) when some of these coefficients are zero. Algorithm 1 shows how to compute the correct PRA ψ in all circumstances, including cases in which Equations (17) and (19) are singular.

Keep-out zone

The keep-out zone for the thermal-sensitive panel is expressed by Equation (5), where ${}^{\mathcal{R}}\hat{\mathbf{h}}_2$ is the panel-normal heading in body/reference frame coordinates, and ${}^{\mathcal{N}}\hat{\mathbf{h}}_{R2} = -{}^{\mathcal{N}}\hat{\mathbf{s}}$. Following the same procedure outlined for Equations (12) and (13), one obtains the expression:

$$g(t) = \frac{Dt^2 + Et + F}{1 + t^2} \geq \cos \theta \quad (20)$$

where:

$$D = {}^{\mathcal{D}}\hat{\mathbf{s}} \cdot {}^{\mathcal{R}}\hat{\mathbf{h}}_2 - 2 \left({}^{\mathcal{D}}\hat{\mathbf{s}} \cdot {}^{\mathcal{R}}\hat{\mathbf{e}}_\psi \right) \left({}^{\mathcal{R}}\hat{\mathbf{h}}_2 \cdot {}^{\mathcal{R}}\hat{\mathbf{e}}_\psi \right) \quad (21a)$$

$$E = 2 {}^{\mathcal{R}}\hat{\mathbf{h}}_2 \cdot \left({}^{\mathcal{R}}\hat{\mathbf{e}}_\psi \times {}^{\mathcal{D}}\hat{\mathbf{s}} \right) \quad (21b)$$

$$F = -{}^{\mathcal{D}}\hat{\mathbf{s}} \cdot {}^{\mathcal{R}}\hat{\mathbf{h}}_2. \quad (21c)$$

Algorithm 1 $\psi = \text{optimalPRA}(A, B, C)$

```

 $\Delta = B^2 - 4AC$ 
if  $A = 0$  then
  if  $B = 0$  then
     $\psi = \pi$ 
  else
     $\psi = -2 \arctan(C/B)$ 
  end if
else
  if  $\Delta < 0$  then
    if  $B = 0$  then
      if  $|A| > |C|$  then
         $\psi = 0$ 
      else
         $\psi = \pi$ 
      end if
    else if
       $q = \frac{A-C}{B}$ 
       $t_1 = q + \sqrt{1+q^2}$ 
       $t_2 = q - \sqrt{1+q^2}$ 
       $f_1 = \frac{|At_1^2 + Bt_1 + C|}{1+t_1^2}$ 
       $f_2 = \frac{|At_2^2 + Bt_2 + C|}{1+t_2^2}$ 
      if  $f_1 < f_2$  then
         $\psi = 2 \arctan(t_1)$ 
      else
         $\psi = 2 \arctan(t_2)$ 
      end if
    end if
  else
     $\psi = 2 \arctan \left( \frac{-B \pm \sqrt{B^2 - 4AC}}{2A} \right)$ 
  end if
end if
return( $\psi$ )

```

However, the previous subsection describes how to compute the PRA in order to ensure that the resulting reference attitude yields the maximum power. It has been shown that there can be two different scenarios, depending on whether $\Delta = B^2 - 4AC$ is negative or not. In the first case, there is only one ψ value that maximizes the generated power. In this circumstance it is not possible to further optimize the reference attitude to accommodate the requirement on the thermal-sensitive platform without compromising the ability to generate power, which is already suboptimal. Conversely, when $\Delta > 0$, two solutions exist. Because these two solutions are equivalent in terms of power generation, the solution for which $g(t(\psi)) \geq \cos \theta$ should be chosen. In the scenario when neither solution satisfies the keep-out constraint, the best solution is the one for which $g(t(\psi))$ is higher.

Performance Discussion

An interesting result is derived exploring the space of possible relative orientations between the unit direction vectors involved in this analysis. Let's define β and δ as the angles between the two body-frame directions, and the two inertial-frame directions, respectively, and γ as the incidence angle on the solar arrays, as defined in Figure 1:

$$\beta = \arccos \left({}^B\hat{\mathbf{a}} \cdot {}^B\hat{\mathbf{h}}_1 \right) \quad (22a)$$

$$\delta = \arccos \left({}^{\mathcal{N}}\hat{\mathbf{s}} \cdot {}^{\mathcal{N}}\hat{\mathbf{h}}_{R1} \right) \quad (22b)$$

$$\gamma = \arccos \left({}^{\mathcal{R}}\hat{\mathbf{a}} \cdot {}^{\mathcal{R}}\hat{\mathbf{s}} \right). \quad (22c)$$

Figure 2 shows the angle $\gamma(\beta, \delta)$ for every combination of $(\beta, \delta) \in [0, \pi] \times [0, \pi]$, where γ is derived after computing the optimal reference \mathcal{R} applying Algorithm 1. The central

plateau where $\gamma = 0$ represents the cases for which $\Delta \geq 0$ and two solutions exist for the optimal reference attitude. Conversely, the four regions in which $0 < \gamma \leq \pi/2$ represent suboptimal configurations in which the optimal illumination on the solar arrays cannot be achieved simultaneously with the thruster pointing constraint ($\Delta < 0$). The relation between the angles expressed in Equation (22) is:

$$\gamma = \begin{cases} \frac{\pi}{2} - \beta - \delta & \text{if } 0 \leq \beta \leq \frac{\pi}{2} \text{ and } \delta < \frac{\pi}{2} - \beta \\ -\frac{\pi}{2} - \beta + \delta & \text{if } 0 \leq \beta \leq \frac{\pi}{2} \text{ and } \delta > \beta + \frac{\pi}{2} \\ -\frac{\pi}{2} + \beta - \delta & \text{if } \frac{\pi}{2} < \beta \leq \pi \text{ and } \delta < \beta - \frac{\pi}{2} \\ \beta + \delta - \frac{3}{2}\pi & \text{if } \frac{\pi}{2} < \beta \leq \pi \text{ and } \delta > \frac{3}{2}\pi - \beta \\ 0 & \text{otherwise.} \end{cases} \quad (23)$$

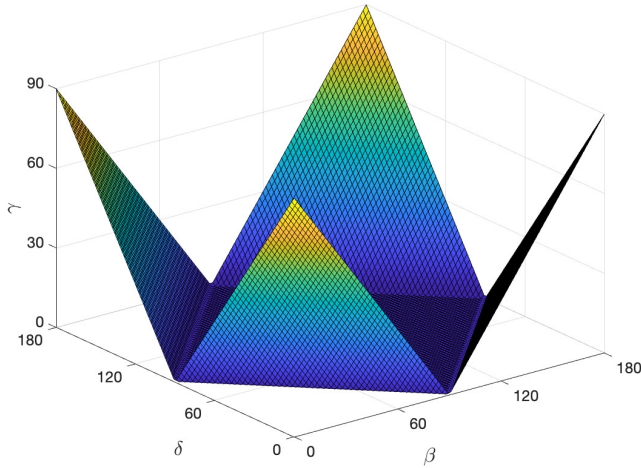


Figure 2: Sun incidence angle on array power-generating surface

Given the parameterization of the problem showed in Equation (13), where the coefficients A , B , and C , depend on the relative headings of two vectors ${}^{\mathcal{R}}\hat{a}$ and ${}^{\mathcal{D}}\hat{s}$ with respect to ${}^{\mathcal{R}}\hat{e}_\psi$. Because each relative heading is characterized by two DoFs, the entire formulation is inherently four-dimensional. However, according to the results in Figure 2, the power performance of the spacecraft parameterized by the resulting incidence angle γ only depends on the two relative angles β and δ .

Based on this results, considerations can be made on the geometry of the spacecraft. For example, Figure 2 shows that when $\beta = \pi/2$ the optimal illumination condition $\gamma = 0$ is always achievable. In a design where the thruster is fixed with respect to the body frame, it is desirable to have the thrust vector perpendicular to the SADA axis: this ensures that the spacecraft can generate the maximum amount of power at all times while thrusting in the right direction. However, when the pointing requirement is driven by a movable component in the \mathcal{B} -frame, like the gimballed thruster, β becomes a function of time, and consequently the optimum γ depends also on δ ,

i.e. the angle between the requested pointing direction and the Sun.

4. INERTIAL POINTING WITH LOWER-BOUNDED POWER GENERATION

This section expands on the earlier results in the following manner. The same set of constraints is considered, but the strict requirement on maximum power generation is relaxed. For a mission to the outer Solar System, the power requirements would be defined based on the arrival conditions, where illumination is worse. However, during flybys of the inner planets, it may not be necessary to use the full power generation capability of the spacecraft and, conversely, it might be more important to ensure that the spacecraft is dissipating heat efficiently. This sections starts from the same initial assumptions of the former one, where the thruster alignment is the main driving requirement for attitude reference generation. Once again, the solution is obtained as the product of two intermediate DCMs as shown in Equation (6). Because power-related considerations do not affect the thruster alignment, the first intermediate DCM $[DN]$ is obtained analogously.

Lower-Bounded Power Generation

When the spacecraft is closer to the Sun, the irradiance on the arrays increases. As a result, more power can be harvested even if the incidence angle of the light on the arrays is not optimal. In such case, the requirement in Equation (3) becomes:

$$-K \leq f(t) \leq K \quad (24)$$

where Equations (12) and (13) still apply, and $K = \sin \gamma$ is a parameter that describes how far off from perpendicular the array surface and sunlight can be while still harvesting a sufficient amount of power. In practice, K constitutes the lower admissible bound on the amount of power that can be generated by the spacecraft in that position in orbit. Because $0 \leq \gamma \leq \pi/2$, it is $0 \leq K \leq 1$, where $K = 0$ means that the lower bound is the maximum power requirement described in the previous section. In practical terms, a limit on how much K should be increased is posed by the shadowing of the spacecraft onto the arrays, which occurs when the SADAs are not perfectly orthogonal to the sunline and further degrades the power-generating performance. Because this issue is specific to the spacecraft design, it is not considered in the following analysis.

Before diving into the discussion of the problem presented by Equation (24), a simplifying assumption is made. No a priori knowledge is given on the coefficients A , B , and C . However, it is possible to assume, without loss of generality, that $A > 0$. This is true because, even when $A < 0$, Equation (24) can be rewritten in an equivalent form where the coefficient of the t^2 term is positive. With this consideration, Equation (24) is rewritten as the system:

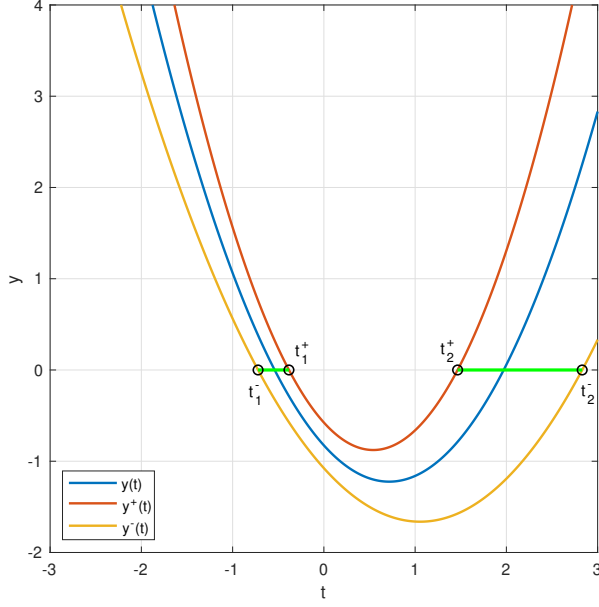
$$\begin{cases} (A + K)t^2 + Bt + (C + K) \geq 0 \\ (A - K)t^2 + Bt + (C - K) \leq 0 \end{cases} \quad (25)$$

with $A \geq 0$ and $0 \leq K \leq 1$. To analyze the solutions of this system it is useful to define the functions:

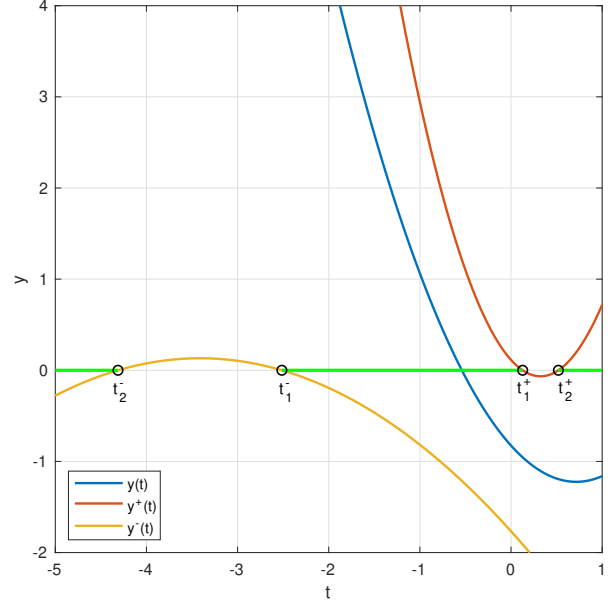
$$y(t) = At^2 + Bt + C \quad (26a)$$

$$y^+(t) = (A + K)t^2 + Bt + (C + K) \quad (26b)$$

$$y^-(t) = (A - K)t^2 + Bt + (C - K) \quad (26c)$$



(a) $K = 0.25$



(b) $K = 0.94$

Figure 3: Solution space with $A = 0.777$, $B = -1.112$, $C = -0.826$

which describe three parabolas as functions of t . It is easy to show that these three parabolas never intersect, except for the case $K = 0$, for which they coincide. Moreover, it is true for any real value of t , that:

$$y^-(t) \leq y(t) \leq y^+(t) \quad (27)$$

Analytical methods can be derived to compute the solution space for the system in Equation (25). These methods are differentiated depending on the sign of the discriminant of the base parabola $y(t)$. The following discriminants are defined for the three parabolas in Equation (26):

$$\Delta = B^2 - 4AC \quad (28a)$$

$$\Delta^+ = B^2 - 4(A + K)(C + K) \quad (28b)$$

$$\Delta^- = B^2 - 4(A - K)(C - K). \quad (28c)$$

• Case $\Delta \geq 0$: the equation $y(t) = 0$ has two solutions. It is interesting to determine for which values of K $y^+(t) = 0$ and $y^-(t) = 0$ also have solutions. Such values are determined by the solution of the following inequality:

$$\begin{aligned} \Delta^\pm &= B^2 - 4(A \pm K)(C \pm K) \geq 0 \\ &= -[4K^2 \pm 4(A + C)K - B^2 + 4AC] \geq 0 \end{aligned} \quad (29)$$

whose discriminant, as a function of the variable K , is:

$$\Delta_K = 16[(A - C)^2 + B^2] \geq 0 \quad (30)$$

and whose critical K values are:

$$K_{1/2}^+ = \frac{-(A + C) \pm \sqrt{(A - C)^2 + B^2}}{2} \quad (31a)$$

$$K_{1/2}^- = \frac{+(A + C) \pm \sqrt{(A - C)^2 + B^2}}{2}. \quad (31b)$$

For both these pairs of solutions it is true that:

$$K_1^\pm \cdot K_2^\pm = -\frac{1}{4}(B^2 - 4AC) \leq 0, \quad (32)$$

from which it can be concluded that each pair of solutions consists of a positive and a negative solution. Based on this result, it is concluded that the conditions for $y^+(t) = 0$ and $y^-(t) = 0$ to have each two solutions are, respectively:

$$K \leq \frac{\sqrt{(A - C)^2 + B^2} - (A + C)}{2} \quad (33a)$$

$$K \leq \frac{\sqrt{(A - C)^2 + B^2} + (A + C)}{2}. \quad (33b)$$

Defining the following zeroes of Equation (26):

$$t_1^+ = \frac{-B - \sqrt{\Delta^+}}{2(A + K)} \quad t_2^+ = \frac{-B + \sqrt{\Delta^+}}{2(A + K)} \quad (34a)$$

$$t_1^- = \frac{-B - \sqrt{\Delta^-}}{2(A - K)} \quad t_2^- = \frac{-B + \sqrt{\Delta^-}}{2(A - K)} \quad (34b)$$

it is possible to visualize the problem represented by Equation (25) in Figure 3, where the solution space is highlighted in green. Attention should be paid to the fact that the parabola $y^-(t)$ changes its concavity depending on the sign of $(A - K)$, and the solution space changes accordingly, as highlighted by the differences between Subfigures (a) and (b). In the event of $K = A$, $y^-(t)$ degenerates into a line, and $t_2^- \rightarrow \infty$. Mapping the solution space in t to the respective PRA gives the range of angles ψ that satisfy Equation (25). Figure 4 shows such solution space for varying values of K , where it is observed that, for $K = 0$, the solution space degenerates into the two individual solutions presented in Equation (17).

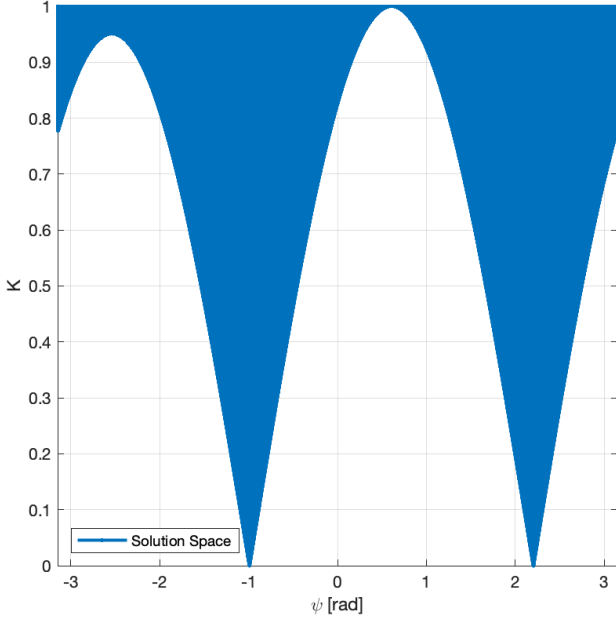


Figure 4: Solution space with $A = 0.777$, $B = -1.112$, $C = -0.826$, $0 \leq K \leq 1$

• Case $\Delta < 0$: the equation $y(t) = 0$ has no real solutions. Based on Equation (27) it is true that $0 < y(t) \leq y^+(t)$, therefore the system in Equation (25) reduces to:

$$y^-(t) = (A - K)t^2 + Bt + (C - K) \leq 0. \quad (35)$$

The discriminant of this equation is expressed by Equation (29), with the negative sign. The two solutions $K_{1/2}^-$ are those in Equation (31b). However, in this case it is:

$$K_1^- \cdot K_2^- = -\frac{1}{4}(B^2 - 4AC) > 0, \quad (36)$$

from which it follows that the two critical K values have the same sign. It can be concluded that $y^-(t) = 0$ has no solutions for $K < K_1^-$, two solutions for $K_1^- \leq K \leq K_2^-$, and infinite solutions for $K > K_2^-$. This result allows to solve Equation (35) and, mapping the solutions for t to the respective PRV values ψ , the solution space in Figure 5 is obtained. Note that, for $K \leq K_1^- = 0.454$, the solution from Equation (19) is chosen to ensure that $|f(t(\psi))|$ is minimum. Analogously, this choice drives the SADA drive axis as close to perpendicularity to sunlight as possible. For $K \geq K_2^- = 0.891$, infinite solutions exist.

Algorithm 2 shows how to derive the solution space Ψ for any combination of A , B , C , and K , and obtain the solution space plots in Figures 4 and 5.

Keep-out zone

For the keep-out constraint, the Equations (20) and (21) still apply. Specifically, Equation (20) can be rewritten in the form:

$$z(t) = (D - Q)t^2 + Et + (F - Q) \geq 0, \quad (37)$$

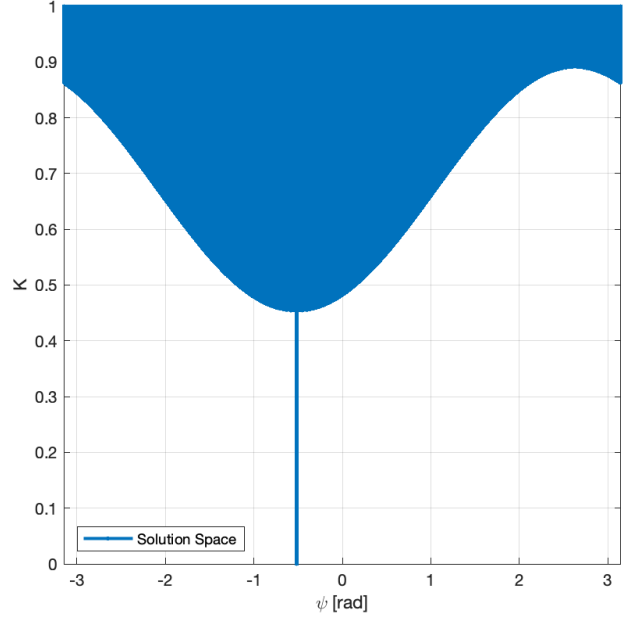


Figure 5: Solution space with $A = -0.863$, $B = -0.216$, $C = -0.483$, $0 \leq K \leq 1$

where $Q = \cos \theta$. The solution set Θ of this inequality can be computed using Algorithm 3. When the set that satisfies Equation (37) is the empty set, the solution computed by Algorithm 3 coincides with the value for which $|z(t)|$ is minimum, i.e., the computed PRA gets the heading \hat{h}_2 as far from the Sun direction as possible.

The final solution of the attitude reference generation problem as a whole is, in this case, the intersection space of Ψ and Θ . A non-empty intersection space contains the solutions that best satisfy all three pointing requirements in order of priority. Conversely, an empty solution space means that it is not possible to satisfy the second and third constraint simultaneously. In this circumstance, it is recommendable to choose ψ such that:

$$\psi \in \Psi : \psi = \arg \min(\text{dist}(\Psi, \Theta)) \quad (38)$$

which means, ψ is the element of the set Ψ that is closest to the set Θ .

5. SOLAR ARRAY REFERENCE GENERATION

Maximum power generation

Once the reference attitude \mathcal{R} is computed, defining the rotation angle for the solar arrays is a relatively trivial problem. The rotation angle of the arrays α is defined with respect to a zero direction, for which $\alpha = 0$. Such direction \hat{b} is fixed in body-frame coordinates and is, by definition, orthogonal to the SADA axis \hat{a} . The goal of this section is to identify the reference direction \hat{b}_R along which the power-generating surface of the solar arrays needs to be pointed. Under the assumption that the requirement is to generate as much power on the solar arrays as possible, the reference \hat{b}_R direction needs to be a linear combination of the SADA axis \hat{a} and the Sun direction vector \hat{s} , and simultaneously orthogonal to

Algorithm 2 $\Psi = \text{SolutionSpaceLB}(A, B, C, K)$

```
if  $A < 0$  then
   $A = -A$ 
   $B = -B$ 
   $C = -C$ 
end if
 $\Delta = B^2 - 4AC$ 
 $\Delta^+ = B^2 - 4(A + K)(C + K)$ 
 $\Delta^- = B^2 - 4(A - K)(C - K)$ 
 $\psi_1^+ = 2 \arctan\left(\frac{-B - \sqrt{\Delta^+}}{2(A + K)}\right)$ 
 $\psi_2^+ = 2 \arctan\left(\frac{-B + \sqrt{\Delta^+}}{2(A + K)}\right)$ 
 $\psi_1^- = 2 \arctan\left(\frac{-B - \sqrt{\Delta^-}}{2(A - K)}\right)$ 
 $\psi_2^- = 2 \arctan\left(\frac{-B + \sqrt{\Delta^-}}{2(A - K)}\right)$ 
 $\psi^- = 2 \arctan\left(\frac{A - C}{B}\right)$ 
if  $\Delta > 0$  then
  if  $K > A$  then
    if  $\Delta^+ \geq 0$  and  $\Delta^- \geq 0$  then
       $\Psi = [\psi_1^-, \psi_1^+] \cup [\psi_2^+, \psi_2^-]$ 
    else if  $\Delta^+ < 0$  and  $\Delta^- \geq 0$  then
       $\Psi = [\psi_1^-, \psi_2^-]$ 
    else
       $\Psi = \emptyset$ 
    end if
  else if  $K = A$  then
    if  $\Delta^+ > 0$  then
       $\Psi = [-\pi, \psi_1^+] \cup [\psi_2^+, \psi^-]$ 
    else
       $\Psi = [-\pi, \psi^-]$ 
    end if
  else
    if  $\Delta^+ \leq 0$  and  $\Delta^- \geq 0$  then
      if  $B < 0$  then
         $\Psi = [-\pi, \psi_2^-] \cup [\psi_1^-, \psi_1^+] \cup [\psi_2^+, \pi]$ 
      else
         $\Psi = [-\pi, \psi_1^+] \cup [\psi_2^+, \psi_2^-] \cup [\psi_1^-, \pi]$ 
      end if
    else if  $\Delta^+ \leq 0$  and  $\Delta^- \geq 0$  then
       $\Psi = [-\pi, \psi_2^-] \cup [\psi_1^-, \pi]$ 
    else if  $\Delta^+ > 0$  and  $\Delta^- < 0$  then
       $\Psi = [-\pi, \psi_1^+] \cup [\psi_2^+, \pi]$ 
    else
       $\Psi = [-\pi, \pi]$ 
    end if
  end if
end if
else
   $\psi_{\min} = \text{optimalPRA}(A, B, C)$ 
  if  $K < A$  then
    if  $\Delta^- < 0$  then
       $\Psi = [\psi_{\min}, \psi_{\min}]$ 
    else
       $\Psi = [\psi_1^-, \psi_2^-]$ 
    end if
  else if  $K = A$  then
     $\Psi = [-\pi, \psi^-]$ 
  else
     $\Psi = [-\pi, \psi_2^-] \cup [\psi_1^-, \pi]$ 
  end if
end if
return( $\Psi$ )
```

$\hat{\mathbf{a}}_.$. This gives the following:

$$\mathcal{R}\hat{\mathbf{b}}_R = \frac{\mathcal{R}\hat{\mathbf{s}} - (\mathcal{R}\hat{\mathbf{a}} \cdot \mathcal{R}\hat{\mathbf{s}})\mathcal{R}\hat{\mathbf{a}}}{\sqrt{1 - (\mathcal{R}\hat{\mathbf{a}} \cdot \mathcal{R}\hat{\mathbf{s}})^2}}. \quad (39)$$

From Equation (39) it is easy to show that $\hat{\mathbf{b}}_R \perp \hat{\mathbf{a}}$ and $\hat{\mathbf{b}}_R \cdot \hat{\mathbf{s}} = \cos \gamma$, where γ is consistent with the definition given in Equation (3). Therefore for $\gamma = 0$, assuming that a solution that satisfies the attitude requirement exists, results in $\hat{\mathbf{b}}_R \parallel \hat{\mathbf{s}}$, that is the arrays are directly facing the Sun. The

Algorithm 3 $\Theta = \text{SolutionSpaceKO}(D, E, F, Q)$

```
 $\theta_{\min} = \text{optimalPRA}(D, E, F)$ 
 $\Delta_{\text{KO}} = D^2 - 4(D - Q)(F - Q)$ 
if  $D = Q$  then
  if  $E = 0$  and  $F \geq Q$  then
     $\Theta = [-\pi, \pi]$ 
  else if  $E = 0$  and  $F < Q$  then
     $\Theta = [\theta_{\min}, \theta_{\min}]$ 
  else if  $E > 0$  then
     $\Theta = \left[2 \arctan\left(\frac{Q - F}{E}\right), \pi\right]$ 
  else
     $\Theta = \left[-\pi, 2 \arctan\left(\frac{Q - F}{E}\right)\right]$ 
  end if
else
  if  $\Delta_{\text{KO}} < 0$  and  $D > Q$  then
     $\Theta = [-\pi, \pi]$ 
  else if  $\Delta_{\text{KO}} < 0$  and  $D < Q$  then
     $\Theta = [\theta_{\min}, \theta_{\min}]$ 
  else
     $\theta_1 = 2 \arctan\left(\frac{-E - \sqrt{\Delta_{\text{KO}}}}{2(D - Q)}\right)$ 
     $\theta_2 = 2 \arctan\left(\frac{-E + \sqrt{\Delta_{\text{KO}}}}{2(D - Q)}\right)$ 
    if  $D > Q$  then
       $\Theta = [-\pi, \theta_1] \cup [\theta_2, \pi]$ 
    else
       $\Theta = [\theta_2, \theta_1]$ 
    end if
  end if
end if
return( $\Theta$ )
```

reference angle for the solar arrays is:

$$\alpha_R = \arccos(\hat{\mathbf{b}} \cdot \hat{\mathbf{b}}_R). \quad (40)$$

Upper-Bounded Power Generation

The case may exist where, due to close proximity to the Sun, the desire is to limit the exposure of the arrays to the Sun. This can happen, for example, to avoid overheating the spacecraft. Effectively, this translates into the problem of upper-bounding the amount of power that can be generated by the arrays. This can be accomplished via two different approaches. With respect to Equation (24), it is possible to redefine the requirement as:

$$H \leq |f(t)| \leq K. \quad (41)$$

This equation can be translated to a problem similar to that analyzed in Section 4, with the difference that, in this case, the solution space would be a subset of the respective solution spaces shown in Figures 4 and 5. Besides the analytical complexity of determining the solution of this problem, this is not the desirable approach because it would ultimately involve computing a new reference frame and slewing the spacecraft to it. The better approach consists in only articulating the solar arrays in order to face them away from sunlight whenever needed. This allows to hold the hub's attitude steady and at the same time change the condition of illumination while only rotating the arrays. Let's define σ as the desired angle between the Sun direction and the normal to the array surface, as opposed to γ , which indicates the smallest such angle possible given the current spacecraft attitude. The relation between the two is:

$$\cos \sigma = \cos \gamma \cos \epsilon, \quad (42)$$

which implies that $\sigma \geq \gamma$. Combining this relation with the result of the previous subsection gives:

$$\begin{aligned}\alpha_R &= \arccos(\hat{\mathbf{b}} \cdot \hat{\mathbf{b}}_R) \pm \epsilon \\ &= \arccos(\hat{\mathbf{b}} \cdot \hat{\mathbf{b}}_R) \pm \arccos\left(\frac{\cos \sigma}{\cos \gamma}\right)\end{aligned}\quad (43)$$

where the same reference angle computed in Equation (40) is offset by an amount ϵ depending on the desired performance. It can be observed that for $\sigma = \gamma$, i.e., when the requirement coincides with the best performance, Equations (40) and (43) coincide. The angles γ , ϵ , σ and α_R are visualized in Figure 6.

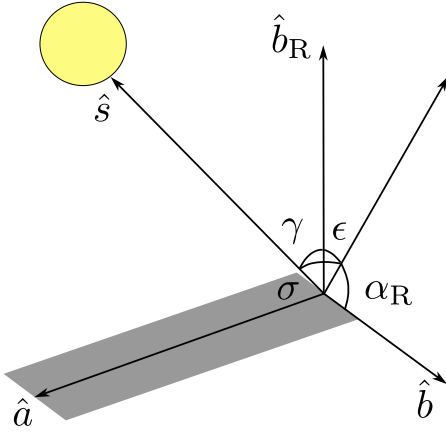


Figure 6: Array reference angles

6. CONCLUSIONS

This paper has presented the problem of defining the reference frame for a spacecraft subject to multiple pointing constraints. Such constraints are represented by, in order of importance, 1. boresight alignment, 2. Sun incidence on the rotating solar arrays, and 3. soft keep-in or keep-out pointing zone. These constraints are relatively common modern spacecraft designs, and this paper provided a detailed description of the attitude spaces of compliant solutions to satisfy most of such requirements simultaneously, or following and ordered priority list.

The first main contribution of this paper is a thorough analysis of the types of constraints that can be met simultaneously given a certain spacecraft design. The results show that, under the assumption that the first requirements is always met, the second requirement can also be achieved when the geometry of the spacecraft is favorable. In this case, two solutions exist that can accommodate the first two requirements simultaneously, and between which it is possible to choose in order to obtain the best result for the third requirement. Conversely, when the solar array requirement cannot be met, a closest solution is derived. Because such a solution is unique, it does not leave any room for further optimization. These results have been expanded to show how, when the Sun incidence requirement is relaxed, the two solutions mentioned above expand into two compliant solution spaces, until eventually merging together. Lastly, attention is paid to how to define the appropriate reference angle for the solar arrays, in order to ensure that the power performances meet the requirements at all times.

The second main contribution of this paper consists in the formulation of the attitude reference problem in terms of the spacecraft geometry and sensor measurements of the sun vector. The fully analytical nature of this formulation makes it noteworthy for on-board implementation, where the attitude reference generation algorithm can be run online, finding the optimal attitude reference for multiple pointing constraints simultaneously with minimal computational burden.

REFERENCES

- [1] K. Holste, P. Dietz, S. Scharmann, K. Keil, T. Henning, D. Zschätzsch, M. Reitemeyer, B. Nauschütt, F. Kiefer, F. Kunze, *et al.*, “Ion thrusters for electric propulsion: Scientific issues developing a niche technology into a game changer,” *Review of Scientific Instruments*, vol. 91, no. 6, p. 061101, 2020.
- [2] E. M. Petro and R. J. Sedwick, “Survey of moderate-power electric propulsion systems,” *Journal of Spacecraft and Rockets*, vol. 54, no. 3, pp. 529–541, 2017.
- [3] M. D. Rayman and D. H. Lehman, “Deep space one: Nasa’s first deep-space technology validation mission,” *Acta Astronautica*, vol. 41, no. 4-10, pp. 289–299, 1997.
- [4] M. Yoshikawa, J. Kawaguchi, A. Fujiwara, and A. Tsuchiyama, “The hayabusa mission,” in *Sample return missions*, pp. 123–146, Elsevier, 2021.
- [5] Y. Tsuda, M. Yoshikawa, M. Abe, H. Minamino, and S. Nakazawa, “System design of the hayabusa 2—asteroid sample return mission to 1999 ju3,” *Acta Astronautica*, vol. 91, pp. 356–362, 2013.
- [6] G. Racca, A. Marini, L. Stagnaro, J. Van Dooren, L. Di Napoli, B. Foing, R. Lumb, J. Volp, J. Brinkmann, R. Grünagel, *et al.*, “Smart-1 mission description and development status,” *Planetary and space science*, vol. 50, no. 14-15, pp. 1323–1337, 2002.
- [7] M. D. Rayman, T. C. Fraschetti, C. A. Raymond, and C. T. Russell, “Dawn: A mission in development for exploration of main belt asteroids Vesta and Ceres,” *Acta Astronautica*, vol. 58, no. 11, pp. 605–616, 2006.
- [8] A. Loehberg, C. Gruenwald, J. Birkel, A. Brandl, N. Kuebler, H. Perrin, T. Andreev, U. Schuhmacher, and S. Taylor, “The BepiColombo Mercury planetary orbiter (MPO) solar array design, major developments and qualification,” in *E3S Web of Conferences*, vol. 16, p. 04006, EDP Sciences, 2017.
- [9] D. Y. Oh, S. Collins, D. Goebel, B. Hart, G. Lantoiné, S. Snyder, G. Whiffen, L. Elkins-Tanton, P. Lord, Z. Pirkel, *et al.*, “Development of the Psyche mission for NASA’s discovery program,” in *35th International Electric Propulsion Conference*, (Atlanta, GA), October 8–12 2017.
- [10] G. Racca, G. Whitcomb, and B. Foing, “The SMART-1 mission,” *ESA bulletin*, vol. 95, pp. 72–81, 1998.
- [11] R. Calaon, L. Kiner, C. Allard, and H. Schaub, “Momentum management of a spacecraft equipped with a dual-gimballed electric thruster,” in *AAS Guidance and Control Conference*, (Breckenridge, CO), Feb. 2–8 2023. Paper No. AAS-23-178.
- [12] T. Bondo, R. Walker, A. Willig, A. Rathke, D. Izzo, and M. Ayre, “Preliminary design of an advanced mission to pluto,” in *24th International Symposium on Space Technology and Science*, Miyazaki, Japan, 2004.

- [13] C. Casaregola, K. Geurts, P. Pergola, and M. Andrenucci, "Radioisotope low-power electric propulsion missions to the outer planets," in *43rd AIAA/ASME/SAE/ASEE Joint Propulsion Conference & Exhibit*, p. 5234, 2007.
- [14] R. Calaon, E. Fantino, R. Flores, and J. Peláez, "Design of the trajectory of a tether mission to Saturn," in *8th European Conference for Aeronautics and Aerospace Sciences (EUCASS)*, 2019.
- [15] B. Heinrich, J. Zemann, and F. Rottmeier, "Development of the BepiColombo MPO solar array drive assembly (SADA)," in *European Space Mechanisms and Tribology Symposium (ESMATS)*, vol. 87, pp. 1–21, 2011.
- [16] A. Boca, C. MacFarland, and R. Kowalczyk, "Solar power for deep-space applications: state of art and development," in *AIAA Propulsion and Energy 2019 Forum*, p. 4236, 2019.
- [17] H. Schaub and J. L. Junkins, *Analytical Mechanics of Space Systems*. AIAA, 4 ed., 2018. Chapter 3, pp. 99–121.

lead in the CICERO mission, the ADCS algorithm lead on a Mars mission and supporting ADCS for a new asteroid mission. He has been awarded the H. Joseph Smead Faculty Fellowship, the Provost's Faculty Achievement Award, the faculty assembly award for excellence in teaching, as well as the Outstanding Faculty Advisor Award. He is a fellow of AIAA and AAS, and has won the AIAA/ASEE Atwood Educator award, AIAA Mechanics and Control of Flight award, as well as the Collegiate Educator of the Year for the AIAA Rocky Mountain section.

BIOGRAPHY



Riccardo Calaon received his B.S. and M.S. degrees in Aerospace Engineering from the University of Padua, Italy, in 2017 and 2019 respectively. He is currently a Ph.D. Candidate and a Fulbright Fellow in the Autonomous Vehicle Systems Lab at CU Boulder, under the supervision of Dr. Hanspeter Schaub, whose team he joined in August 2020. His current research focuses on GN&C

and planning algorithms applied to the field of attitude dynamics for spacecraft with complex pointing constraints.



Cody Allard is a Guidance, Navigation and Control Engineer at the Laboratory for Atmospheric and Space Physics at the University of Colorado - Boulder. He received a PhD in Aerospace Engineering Sciences from the University of Colorado - Boulder, a BS in Mechanical Engineering, a BS in Physics and a MS in Mechanical & Aerospace Engineering from the University of Missouri -

Columbia. His research interests include attitude dynamics and control, payload pointing and control, simulation software architecture and general multi-body dynamics.



Hanspeter Schaub is a professor and chair of the University of Colorado aerospace engineering sciences department. He holds the Schaden leadership chair. He has over 28 years of research experience, of which 4 years are at Sandia National Laboratories. His research interests are in astrodynamics, relative motion dynamics, charged spacecraft motion as well as spacecraft autonomy.

This has led to about 207 journal and 332 conference publications, as well as a 4th edition textbook on analytical mechanics of space systems. Dr. Schaub has been the ADCS